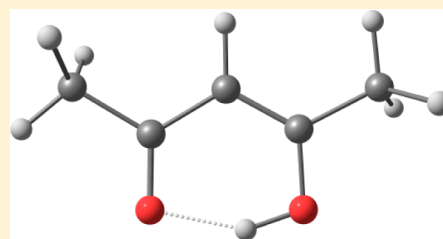


Tautomeric Properties and Gas-Phase Structure of Acetylacetone

Natalya V. Belova,^{*,†} Heinz Oberhammer,[‡] Nguen Hoang Trang,[†] and Georgiy V. Girichev[†][†]Research Institute for Thermodynamics and Kinetics of Chemical Processes, Ivanovo State University of Chemistry and Technology, 153460 Ivanovo, Russia[‡]Institut für Physikalische und Theoretische Chemie, Universität Tübingen, 72076 Tübingen, Germany

S Supporting Information

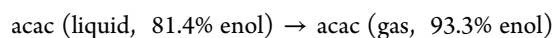
ABSTRACT: The tautomeric and structural properties of acetylacetone, $\text{CH}_3\text{C}(\text{O})\text{CH}_2\text{C}(\text{O})\text{CH}_3$, have been studied by gas-phase electron diffraction (GED) and quantum chemical calculations (B3LYP and MP2 approximation with different basis sets up to aug-cc-pVTZ). The analysis of GED intensities resulted in the presence of 100(3)% of the enol tautomer at 300(5) K and 64(5)% of the enol at 671(7) K. The enol tautomer possesses C_s symmetry with a planar ring and strongly asymmetric hydrogen bond. The diketo form possesses C_2 symmetry. The experimental geometric parameters of both tautomeric forms are reproduced very closely by B3LYP/aug-cc-pVTZ and MP2/cc-pVTZ methods.



■ INTRODUCTION

Over many years, β -diketones (β -dicarbonyl compounds) have been of considerable interest to organic, inorganic, and physical chemistry because a large group of the applications of these compounds concerns their role as important organic reagents.^{1–4} β -Diketones were found to be useful chelating ligands as well. The possibility of diketo–enol tautomerization, the conformational and structural properties of β -diketones, and the nature of the strong intramolecular O–H...O hydrogen bond in the enol form have also attracted special attention.

Acetylacetone (acac, $\text{CH}_3\text{C}(\text{O})\text{CH}_2\text{C}(\text{O})\text{CH}_3$) has been a subject of numerous studies, both experimental and theoretical. However, the detailed tautomeric and conformational properties of acac are not yet clear. Acetylacetone is known to exist in two forms, i.e. diketo and enol, but rather different relative concentrations of these two tautomers have been reported in the literature. It is well-known that the preference for the enol or diketo form depends strongly on temperature, solvent, and phase.³ Numerous NMR studies^{5–9} show strong predominance of the enol tautomer from 81% in pure liquid⁸ to 95% in CCl_4 solution.⁹ On the other hand, the percentage of the enol form in DMSO is only 63%⁹ and is even less (17%) in water.¹⁰ These results can be compared with an FT-IR study of tautomeric properties of acac in different solvents,¹¹ where the highest enol concentration (86%) was observed in CCl_4 and the highest contribution of the diketo tautomer (48%) was in DMSO. Temprado et al.¹² point out that the enol tautomer is more volatile and therefore its concentration in the gas phase has to be even higher than that in a liquid (81%). Using the experimental enthalpy of vaporization (10.0 ± 0.1 kcal/mol) for the evaporation process at 25 °C, Irving and Wadso¹³ derived the tautomeric composition of acac in a gas phase:



¹H NMR studies¹⁴ show that the enol form of acac predominates in the liquid, solution, and gas phases at all temperatures under investigation. From the experimental gas-phase data in 373–445 K temperature range the values of $\Delta H^\circ = H^\circ_{\text{keto}} - H^\circ_{\text{enol}} = 4.66(18)$ kcal/mol and $\Delta S^\circ = 8.26(45)$ cal/(mol K) were derived. The extrapolated value for $\Delta G^\circ_{298} = 2.20(45)$ kcal/mol leads to a 2.5(13)% concentration of the diketo tautomer at 298 K. On the other hand, about 10% of the diketo form was derived from xenon matrix FT-IR spectra of acac at 10 K.¹⁵ This result was not confirmed by later studies,^{16,17} where only about 1% of the diketo form of acac was found in a neon matrix. From photoelectron spectra at different temperatures¹⁸ the equilibrium constants for the diketo \leftrightarrow enol reaction in the gas phase and its temperature dependence have been obtained. From the values of the equilibrium constants¹⁸ enol concentrations of 73% at 25 °C, 60% at 100 °C, and about 50% at 175 °C have been derived.

According to different quantum chemical calculations a diketo \leftrightarrow enol equilibrium for acetylacetone has to be shifted strongly toward the enol form. Ab initio calculations based on a complete basis set (CBS) extrapolation procedure¹⁹ using B3LYP-cc-pVTZ structures result in tautomerization enthalpy $\Delta H(\text{enol} \rightarrow \text{keto})$ value of 3.27 kcal/mol. CBS-4 calculations²⁰ performed for acac lead to a $\Delta G^\circ_{298} = G^\circ_{\text{keto}} - G^\circ_{\text{enol}} = 2.65$ kcal/mol value and only 1.1% content of the diketo form at 298 K. The calculations (DFT/B3LYP)²¹ predict $\Delta G^\circ_{298} = 3.95$ kcal/mol and an even stronger predominance of the enol tautomer (only 0.1% of the diketo form).

Four different electron diffraction studies of acac have been reported, with rather conflicting results.^{22–25} The experimental intensities recorded at room temperature^{23,24} have been interpreted in terms of the presence of the enol form only. A study performed at 105 °C resulted in an enol contribution of

Received: December 25, 2013

Published: April 23, 2014

$66 \pm 5\%$,²² in good agreement with the value derived from the photoelectron spectra at $100\text{ }^{\circ}\text{C}$ ¹⁸ (see above). An enol contribution of $78 \pm 4\%$ at $155\text{ }^{\circ}\text{C}$ was reported in the most recent GED investigation.²⁵ This value is in agreement with the concentration obtained from gas-phase NMR values (79% enol at $155\text{ }^{\circ}\text{C}$).¹⁴ It should be noted that GED geometries of the enol tautomers reported in refs 22–25 as well as the diketo structures reported in refs 22 and 25 are rather different. In an early study Karle et al.²² found the enol form to possess a symmetric $\text{O}\cdots\text{H}\cdots\text{O}$ bond (C_{2v} overall symmetry) with closely spaced oxygen centers ($r(\text{O}\cdots\text{O}) = 2.381\text{ \AA}$). The same symmetry of the enol form was confirmed by Andreassen et al.²³ However, the distance $r(\text{O}\cdots\text{O}) = 2.519(24)\text{ \AA}$ reported in ref 23 is considerably longer. The enol structure of C_s symmetry was found by Iijima et al.²⁴ as well as by Srinivasan et al.²⁵ in their GED studies. However, the authors of ref 24 proposed a structure with the hydroxyl proton jutting 0.45 \AA out of a molecular plane. Furthermore, the structures of the diketo form reported in refs 22 and 25 are different. In three early GED studies^{22–24} the information from quantum chemical calculations was not used, but such information is of great importance for choosing a correct molecular model, especially in the case of a mixture of two tautomers. In the most recent study²⁵ the diffraction data were recorded with a UED (ultrafast electron diffraction) apparatus with the diffraction angle $s_{\text{max}} = 15\text{ \AA}^{-1}$, which is only about half of that used in conventional GED experiments.

The question about the symmetry of the hydrogen bond in the enol form of acac is widely discussed in the literature (see e.g. ref 26). Numerous quantum chemical calculations at different levels of theory^{26–34} predict a double-well potential surface for proton transfer with the global minimum of energy corresponding to a structure of C_s symmetry and with a symmetric (C_{2v}) transition state. The height of the potential barrier between those two configurations depends on the level of theory. On the other hand, two GED results^{23,24} and a microwave study of acac³⁵ were interpreted in the framework of C_{2v} symmetry of the enol form.

Thus, despite numerous experimental and theoretical investigations, tautomeric and structural properties of acetylacetone still remain a matter of controversy. This fact motivated us to perform a new GED study of acetylacetone at two different temperatures, to determine the tautomeric and structural properties of acac at room temperature and their variation at higher temperature.

■ QUANTUM CHEMICAL CALCULATIONS

All quantum chemical calculations in the present study were performed using the GAUSSIAN03 program set.³⁶ To detect all possible diketo conformers of acac, the two-dimensional potential energy surface has been scanned with the B3LYP/6-31G(d,p) method. The torsion angles $\tau(\text{O1C2C1C3})$ and $\tau(\text{O2C3C1C2})$ were varied in steps of 20° with full optimization of all other parameters (see Figure 1 for atom numbering). This surface possesses only one minimum for the *sc,sc* conformer (*sc* = synclinal orientation of $\text{C}=\text{O}$ bond). The calculated potential surface (with B3LYP/6-31G(d,p)) for rotation of methyl groups in the enol form of acac possesses the minimum energy corresponding to the conformer shown in Figure 1. Methyl groups eclipse the adjacent $\text{C}=\text{C}$ and $\text{C}=\text{O}$ double bonds, respectively. The geometries of both diketo and enol tautomers were fully optimized with B3LYP and MP2 methods with different basis sets. All geometric parameters of

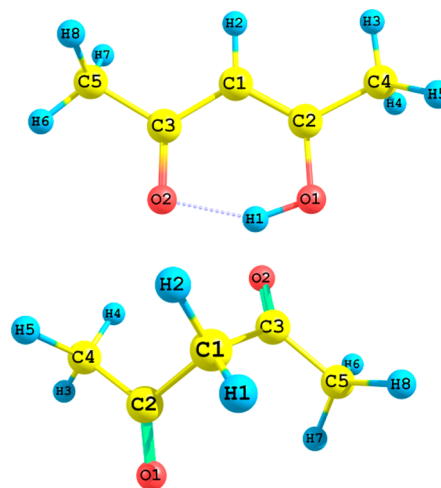


Figure 1. Molecular structures of the enol (top) and diketo (bottom) forms of acetylacetone.

two tautomeric forms obtained with different methods are very close. Harmonic vibrational frequencies were calculated for all optimized geometries in order to confirm that they correspond to a stationary point and to calculate zero point energy (ZPE) corrections and mole fractions of the conformers in the gas phase at different temperatures. The thermodynamic functions required to calculate the mole fractions were estimated with the harmonic oscillator–rigid rotator approximation for a partition function.

The relative energies ($\Delta E = E_{\text{keto}} - E_{\text{enol}}$) and relative free energies ($\Delta G^{\circ}_{298} = G^{\circ}_{\text{keto}} - G^{\circ}_{\text{enol}}$) obtained with the different computational methods as well as the contents of the two tautomeric forms at 298 and 671 K are summarized in Table 1 along with the dihedral angles.

The values in Table 1 demonstrate that predicted relative energies of diketo and enol tautomers depend strongly on the computational method. Whereas both B3LYP methods and MP2/cc-pVTZ calculations predict a strong preference for the enol tautomer at room temperature and in overheated vapor, the MP2 method with small basis sets predicts values of $\Delta G^{\circ}_{298} = 0.83\text{ kcal/mol}$ and $\Delta G^{\circ}_{671} = 0.39\text{ kcal/mol}$, which correspond to rather equal amounts of the two tautomers at 671 K.

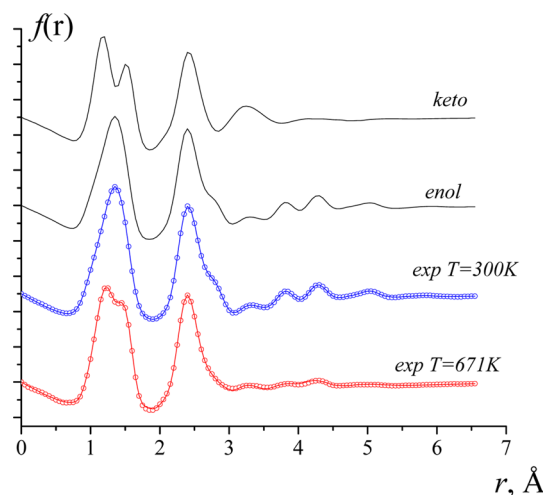
The geometric parameters for the enol and diketo forms which were derived with B3LYP/aug-cc-pVTZ and MP2/cc-pVTZ methods are given in Table 2 together with the experimental results. Vibrational amplitudes and corrections, $\Delta r = r_{\text{h1}} - r_{\text{a}}$, were derived from theoretical force fields (B3LYP/aug-cc-pVTZ) by Sipachev's method (approximation with nonlinear transformation of Cartesian coordinates into internal coordinates), using the program SHRINK.^{37–39} Relevant values for the enol and diketo forms are given in Tables S1 and S2 (Supporting Information), respectively.

■ STRUCTURE ANALYSIS

The heaviest ion in the mass spectra recorded for both experimental series was the parent ion $[\text{C}_5\text{H}_8\text{O}_2]^+$ (Table 5). This proves that only monomers are present in the vapor under the conditions of GED experiments. The experimental radial distribution functions (Figure 2) were derived by Fourier transformations of the experimental intensities. Figure 2 demonstrates that the theoretical radial distribution functions for enol and diketo tautomers of acac differ very strongly.

Table 1. Torsion Angles, Optimized Relative Energies, Gibbs Free Energies at 298 K, and Relative Contents of the Enol and Diketo Tautomers of Acetylacetone at 298 and 671 K

	enol	diketo
B3LYP/6-31G(d,p)		
$\tau(\text{O1C2C1C3})^a$	0	89.1
$\tau(\text{O2C3C1C2})$	0	89.1
$\tau(\text{O1C2C4H3})$	180.0	-7.0
$\tau(\text{O2C3C5H6})$	0.0	-7.0
ΔE , kcal/mol	0	6.48
ΔG°_{298} , kcal/mol	0	5.66
content ($T = 298.25$ K), %	100	0
content ($T = 671$ K), %	98.3	1.7
B3LYP/aug-cc-pVTZ		
$\tau(\text{O1C2C1C3})$	0	88.1
$\tau(\text{O2C3C1C2})$	0	88.1
$\tau(\text{O1C2C4H3})$	180.0	-6.6
$\tau(\text{O2C3C5H6})$	-4.5	-6.6
ΔE , kcal/mol	0	6.24
ΔG°_{298} , kcal/mol	0	5.76
content ($T = 298.25$ K), %	100	0
content ($T = 671$ K), %	97.5	2.5
MP2/6-31G(d,p)		
$\tau(\text{O1C2C1C3})$	0	88.4
$\tau(\text{O2C3C1C2})$	0	88.4
$\tau(\text{O1C2C4H3})$	180.0	-7.0
$\tau(\text{O2C3C5H6})$	0.0	-7.0
ΔE , kcal/mol	0	1.47
ΔG°_{298} , kcal/mol	0	0.83
content ($T = 298.25$ K), %	79.5	20.5
content ($T = 671$ K), %	57.3	42.7
MP2/cc-pVTZ		
$\tau(\text{O1C2C1C3})$	0	88.6
$\tau(\text{O2C3C1C2})$	0	88.6
$\tau(\text{O1C2C4H3})$	180.0	-7.6
$\tau(\text{O2C3C5H6})$	0.0	-7.6
ΔE , kcal/mol	0	4.85
ΔG°_{298} , kcal/mol	0	3.75
content ($T = 298.25$ K), %	99.9	0.1
content ($T = 671$ K), %	94.3	5.7

^aAll values for angles in deg. See Figure 1 for atom numbering.**Figure 2.** Experimental (dots) and calculated radial distribution functions for two experimental series at two temperatures and the theoretical curves for two tautomeric forms.

Differences occur in the region of bonded distances as well as nonbonded distances. The experimental curve obtained at room temperature can be reproduced reasonably well only with the enol tautomer, whereas the experimental $f(r)$ function for overheated vapor cannot be reproduced with a diketo or enol form alone.

In the least-squares analysis a mixture of both diketo and enol forms was considered. For both tautomers the differences between all C–H (and O–H in the enol form) bond lengths, between all C–C bond lengths, and between C–O bond lengths were constrained to calculated values (B3LYP/aug-cc-pVTZ). According to quantum chemical calculations a planar skeleton with overall C_s symmetry of the enol ring was assumed. For the diketo form C_2 symmetry was examined. Starting parameters from B3LYP/aug-cc-pVTZ calculations were refined by a least-squares procedure of the molecular intensities. For the experimental data recorded at room temperature only parameters for the enol form were refined. Independent r_{hl} parameters were used to describe the molecular structure. Vibrational amplitudes were refined in groups with fixed differences. In the analysis for the first experimental series the following correlation coefficients had values larger than 0.8: $\angle \text{C1C2O1}/\angle \text{C1C3O2} = -0.93$ and $\angle \text{C1C2C4}/\angle \text{C1C3C5} = -0.99$. There were only four values of correlation coefficients larger than 0.8 in the high-temperature experimental data analysis: $(\angle \text{C1C2O1}/\angle \text{C1C3O2})_{\text{enol}} = -0.94$, $(\angle \text{C1C2C4}/\angle \text{C1C3C5})_{\text{enol}} = -0.99$, $(\angle \text{H6C5C3})_{\text{enol}}/(\angle \text{C2C1C3})_{\text{keto}} = -0.83$, and $(\angle \text{C2C1C3})_{\text{enol}}/(\angle \text{C1C2O1})_{\text{keto}} = -0.83$.

The best agreement factor ($R_f = 3.6\%$) in the least-squares analysis was for 100(3)% enol at room temperature. A model with a symmetric hydrogen bond and C_{2v} symmetry of the enol skeleton of acac was tested in a GED analysis of room-temperature experimental data. This refinement led to $R_f = 7.6\%$. The statistical Hamilton criterion⁴⁰ at the 0.01 significance level distinctly shows that the model of C_{2v} symmetry must be rejected because the critical value $R_f = 3.78\%$.

Although GED intensities are rather insensitive to the position of the enolic hydrogen atom, C_{2v} and C_s structures differ strongly in their skeletal CC and CO bond distances. Whereas both CC and CO distances are equal in the C_{2v} structure, all of these distances are different in the C_s structure. GED intensities are rather sensitive to these bond distances, resulting in a large difference between the R_f factors. Thus, the GED experiment confirms our quantum chemical calculations, which predict an asymmetric enol structure with a localized O–H bond. A calculated potential function for a hydrogen position between two oxygen atoms is discussed below.

Final results of the least-squares analysis for the enol tautomer for both experimental series are given in Table 2 (structural parameters) and Table S1 (Supporting Information; vibrational amplitudes); the structural parameters and vibrational amplitudes for the diketo form, obtained in the least-squares analysis of high-temperature experimental data, are given in Tables 2 and Table S2 (Supporting Information), respectively. The refined structural parameters are rather similar to those predicted by the quantum chemical calculations.

DISCUSSION

Table 5 and Figure 5 present the mass spectra of acetylacetone, $\text{CH}_3\text{C}(\text{O})\text{CH}_2\text{C}(\text{O})\text{CH}_3$, recorded simultaneously with GED patterns at two different temperatures of the experiment. In a

Table 2. Experimental and Calculated Geometric Parameters of the Enol and Diketo Forms of Acetylacetone^a

	enol				diketo		
	GED ($r_{\text{hl}}, \angle_{\text{hl}}$) ^b		r_e structure		GED ($r_{\text{hl}}, \angle_{\text{hl}}$) ^b $T = 671 \text{ K}$	r_e structure	
	$T = 300 \text{ K}$	$T = 671 \text{ K}$	B3LYP/ aug-cc-pVTZ	MP2/ cc-pVTZ		B3LYP/ aug-cc-pVTZ	MP2/ cc-pVTZ
$r(\text{C1}-\text{C2})$	1.368(3) p_1^c	1.370(3) p_1	1.367	1.366	1.540(4) p_{11}	1.533	1.524
$r(\text{C1}-\text{C3})$	1.441(3) (p_1)	1.443(3) (p_1)	1.440	1.441	1.540(4) (p_{11})	1.533	1.524
$r(\text{C2}-\text{C4})$	1.492(3) (p_1)	1.494(3) (p_1)	1.491	1.488	1.514(4) (p_{11})	1.506	1.502
$r(\text{C3}-\text{C5})$	1.509(3) (p_1)	1.511(3) (p_1)	1.508	1.504	1.514(4) (p_{11})	1.506	1.502
$r(\text{C2}-\text{O1})$	1.326(3) p_2	1.318(4) p_2	1.324	1.325	1.204(4) p_{12}	1.209	1.217
$r(\text{C3}-\text{O2})$	1.248(3) (p_2)	1.240(4) (p_2)	1.245	1.247	1.204(4) (p_{12})	1.209	1.217
$r(\text{C4}-\text{H3})$	1.088(3) p_3	1.094(4) p_3	1.087	1.085	1.093(4) (p_3)	1.087	1.085
$r(\text{C4}-\text{H4})$	1.093(3) (p_3)	1.099(4) (p_3)	1.091	1.089	1.097(4) (p_3)	1.092	1.090
$r(\text{C4}-\text{H5})$	1.093(3) (p_3)	1.099(4) (p_3)	1.091	1.089	1.099(4) (p_3)	1.093	1.091
$r(\text{C5}-\text{H6})$	1.087(3) (p_3)	1.094(4) (p_3)	1.087	1.085	1.093(4) (p_3)	1.087	1.085
$r(\text{C5}-\text{H7})$	1.093(3) (p_3)	1.099(4) (p_3)	1.092	1.090	1.097(4) (p_3)	1.092	1.090
$r(\text{C5}-\text{H8})$	1.093(3) (p_3)	1.099(4) (p_3)	1.092	1.090	1.099(4) (p_3)	1.093	1.091
$r(\text{C1}-\text{H2})$	1.080(3) (p_3)	1.086(4) (p_3)	1.079	1.078	1.095(4) (p_3)	1.088	1.087
$r(\text{O1}-\text{H1})$	1.007(3) (p_3)	1.013(4) (p_3)	1.006	1.006			
$\angle \text{C2C1C3}$	121.1(0.8) p_4	120.0(1.0) p_4	120.8	120.2	108.3(1.5) p_{13}	108.4	105.8
$\angle \text{C1C2O1}$	121.3(1.2) p_5	120.4 (1.3) p_5	121.7	122.0	123.9(2.0) p_{14}	120.6	120.8
$\angle \text{C1C3O2}$	121.0(2.0) p_6	120.3 (1.5) p_6	121.6	121.8	123.9(2.0) (p_{14})	120.6	120.8
$\angle \text{C1C2C4}$	123.5(1.0) p_7	123.6 (1.2) p_7	124.3	124.1	115.3(1.7) p_{15}	116.3	115.7
$\angle \text{C1C3C5}$	119.4(1.0) p_8	118.0 (2.0) p_8	118.7	118.2	115.3(1.7) (p_{15})	116.3	115.7
$\angle \text{C3C1H2}$	119.5(2.1)	120.0(2.2)	119.8	120.2	108.0 ^d	108.0	108.5
$\angle \text{C2C1H2}$	119.5(2.1)	120.0(2.2)	119.4	119.5	110.8 ^d	110.8	111.1
$\angle \text{H3C4C2}$	111.6(1.3) p_9	111.6(1.5) p_9	111.6	111.3	110.3 ^d	110.3	110.3
$\angle \text{H4C4C2}$	109.8(1.3) (p_9)	109.7(1.5) (p_9)	109.7	109.5	110.1 ^d	110.1	109.6
$\angle \text{H6C5C3}$	108.6(1.5) p_{10}	109.9(1.5) p_{10}	109.9	109.8	110.3 ^d	110.3	110.3
$\angle \text{H7C5C3}$	109.0(1.5) (p_{10})	110.3(1.5) (p_{10})	110.3	109.9	110.1 ^d	110.1	109.6
$\angle \text{H4C4H5}$	107.0(2.2)	107.1(2.3)	107.1	107.4	106.8 ^d	106.8	107.1
$\angle \text{H8C5H7}$	111.2(2.0)	107.7(2.1)	107.1	107.4	106.8 ^d	106.8	107.1
$\angle \text{H1O1C2}$	105.9 ^d	105.9 ^d	105.9	104.4			
O1C2C1C3	0.0 ^d	0.0 ^d	0.0	0.0	87.0(8.2)	89.1	88.6
C4C2C1O1	180.0 ^d	180.0 ^d	180.0	180.0	178.4 ^d	178.4	177.3
H6C5C3O2	0.0 ^d	0.0 ^d	0.0	0.0			
H3C4C2C1	0.0 ^d	0.0 ^d	0.0	0.0	171.3 ^d	171.3	169.6
content, %	100(3)	64(5)			36(5)		
symmetry	C_s	C_s	C_s	C_s	C_2	C_2	C_2
R_p %	3.6	3.8			3.8		

^aDistances in Å and angles in degrees. For atom numbering see Figure 1. ^bUncertainties in $r_{\text{hl}} \sigma = (\sigma_{\text{sc}}^2 + (2.5\sigma_{\text{LS}})^2)^{1/2}$ ($\sigma_{\text{sc}} = 0.002r$, σ_{LS} = standard deviation in least-squares refinement) and for angles $\sigma = 3\sigma_{\text{LS}}$. ^c p_i = parameter refined independently. (p_i) = parameter calculated from the independent parameter p_i by the difference $\Delta = p_i - (p_i)$ from the quantum chemical calculations (B3LYP/aug-cc-pVTZ). ^dNot refined.

mass spectrometric study of acetylacetone⁴¹ it was noted that the enolic form contributes significantly to quite a large $[\text{M} - \text{CH}_3]^+$ peak in the mass spectra, whereas the diketo form would be expected to contribute mainly to the McLafferty ($[\text{M} - 42]^+$) peak and in part to the acylium $[\text{CH}_3\text{C}(\text{O})]^+$ ion. Thereby mass spectra in Figure 5 definitely show that the temperature increase favors the diketo form. The GED experiment for acac is consistent with the presence of 100(3)% enol form in the gas phase at 300(5) K. From this GED result only a lower limit for the free energy difference can be derived, $\Delta G_{298}^\circ = G^\circ(\text{keto}) - G^\circ(\text{enol}) > 2.1 \text{ kcal/mol}$. This value is in agreement with the extrapolated free energy difference derived from ^1H NMR spectra ($\Delta G_{298}^\circ = 2.20(45) \text{ kcal/mol}$). Overheating of the acac vapor leads to increasing diketo content. According to GED the tautomeric mixture of acac at 671(7) K consists of 64(5)% enol and 36(5)% diketo form. This composition corresponds to the free energy difference $\Delta G_{671}^\circ = 0.77(21) \text{ kcal/mol}$. This GED result differs considerably from $\Delta G_{671}^\circ = -0.88 \text{ kcal/mol}$, derived

from $\Delta H^\circ = 4.66 \text{ kcal/mol}$ and $\Delta S^\circ = 8.26 \text{ cal/(mol K)}$ obtained from gas-phase NMR data in the temperature range 373–445 K.¹⁴ According to this extrapolated free energy difference the diketo form should be dominant at 671 K. This rather unreasonable result is due to a very large entropy difference ΔS° . Quantum chemical calculations predict much smaller entropy differences between these two tautomers: namely, 1.61 (B3LYP/aug-cc-pVTZ) and 2.19 cal/(mol K) (MP2/cc-pVTZ). A conclusion which is similar to NMR data follows from the photoelectron spectroscopic study,¹⁸ which reports equal contents of two tautomeric forms even at 448 K. Surprisingly, the tautomeric composition and the ΔG_{671}° value derived from GED are reproduced more closely by MP2/6-31G(d,p) calculations ($\Delta G_{671}^\circ = 0.39 \text{ kcal/mol}$), although as we mentioned in previous investigations^{34,42,43} this level of theory usually fails in predicting the tautomeric composition in β -diketones. All other computational methods given in Table 1 predict very low contributions (<6%) of the diketo tautomer at 671 K. This confirms

Table 3. Calculated and Experimental Parameters of Two Tautomeric Forms of Acetylacetone^a

$r(\text{C1}-\text{C2})$	$r(\text{C1}-\text{C3})$	$r(\text{C2}-\text{O1})$	$r(\text{C3}-\text{O2})$	$r(\text{C2}-\text{C4})$	$r(\text{C3}-\text{C5})$	$r(\text{O1}-\text{H})$	$r(\text{O1}\cdots\text{O2})$	$\angle\text{C2C1C3}$	$\angle\text{C1C2O1}$	$\angle\text{C1C3O2}$	T, K	content, %	ref
Enol Form													
1.397(2)	1.283(2)	1.283(2)	1.283(2)	1.486(3)	1.486(3)	0.91(5)	2.541(2)	121.3(2)	121.5(2)	121.5(2)	210	100	X ^b , 44
1.402(1)	1.291(1)	1.291(1)	1.291(1)	1.497(1)	1.497(1)	0.89(3)	2.547(1)	121.2(1)	121.8(1)	121.8(1)	110	100	X ^b , 44
1.416(10)	1.315(7)	1.315(7)	1.315(7)	1.497(10)	1.497(10)		2.381	118.0(2.5)	120.0(1.4)	120.0(1.4)	378	66(5)	GED, (r_e), 22
1.405(5)	1.287(5)	1.287(5)	1.287(5)				2.519(24)	118.3(1.8)	123.2(1.7)	123.2(1.7)	290	~100	GED, (r_e), 23
1.382(7)	1.430(8)	1.319(3)	1.243(2)				2.512(8)	119.7(5)	121.0(8)	123.0(7)	294	~100	GED, (r_e), 24
1.359(34)	1.443(19)	1.321(21)	1.262(5)	1.504(21)	1.518(23)		2.592	120.4(1.0)	123.5	123.1	428	78(4)	GED, (r_e), 25
1.368(3)	1.441(3)	1.326(3)	1.248(3)	1.492(3)	1.509(3)	1.007(3)	2.521(9)	121.1(0.8)	121.3(1.2)	121.0(2.0)	300	100(3)	GED, (r_{h1}), this work
1.370(3)	1.443(3)	1.318(4)	1.240(4)	1.494(3)	1.511(3)	1.013(4)	2.453(15)	120.0(1.0)	120.4(1.3)	120.3(1.5)	671	64(5)	GED, (r_{h1}), this work
1.367	1.440	1.324	1.245	1.491	1.508	1.006	2.531	120.8	121.7	121.6	298	100	calcd ^c , r_e , this work
Diketo Form													
1.540(15)	1.225(10)	1.225(10)	1.225(10)	1.540(15)	1.540(15)		2.767(30)	114.0(3.6)	120.0(1.8)	120.0(1.8)	378	34(5)	GED, (r_e), 22
1.540(4)	1.204(4)	1.204(4)	1.204(4)	1.514(4)	1.514(4)		4.051(43)	108.3(1.5)	123.9(2.0)	123.9(2.0)	671	36(5)	GED, (r_{h1}), this work
1.533	1.209	1.209	1.209	1.506	1.506		4.042	108.4	120.6	120.6	298	<1	calcd ^c , r_e , this work

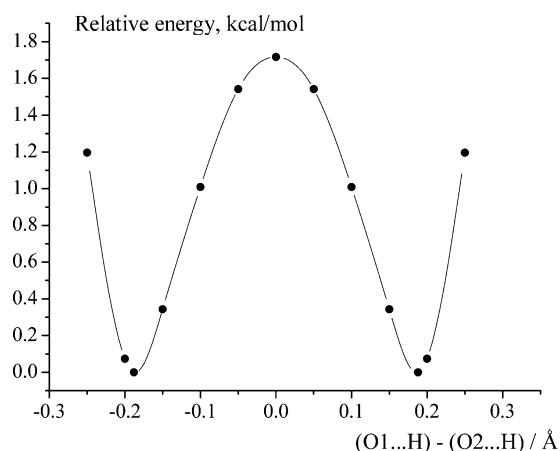
^aFootnote a. ^bFootnote b. ^cFootnote c.

Figure 3. Calculated (B3LYP/6-31G(d,p)) potential curve for the hydrogen atom between the two oxygen atoms in the enol form. The position of the hydrogen atom is described by the difference between O1...H and O2...H distances.

our conclusion that the level of theory for exact predictions of tautomeric compositions obviously should be higher,³⁴ because the accurate calculation of tautomeric composition requires a reliable estimate not only of the energy difference but also of the entropy contribution, which is most important in the case of low vibrational frequencies, such as internal rotation of the methyl groups (19 cm^{-1} from B3LYP/aug-cc-pVTZ and 49 cm^{-1} from MP2/cc-pVTZ).

It should be noted that the enol content reported in previous GED investigations for the vapor phase at 378 K^{22} and 428 K^{25} seems to be underestimated. Moreover, according to the results of refs 22 and 25 the temperature increase leads to a decreasing enol content in the vapor (see Table 3). One of the reasons for such discrepancies of GED results can be explained by different assumptions for enol and diketo geometries used in structural analysis.

Table 2 compares GED and calculated structural parameters obtained in this study for enol and diketo forms, respectively. We can note a good agreement between the experimental and calculated values. The enol tautomer possesses C_s symmetry with a planar ring and asymmetric O-H...O hydrogen bond. The diketo tautomer possesses C_2 symmetry with torsion angles $\text{O1C2C1C3} = \text{O2C3C1C2} = 87.0(8.2)^\circ$.

Table 3 presents the most important geometrical parameters of acac obtained in different investigations for gas-phase and crystal states. As noted above, independent GED studies of acetylacetone resulted in rather different vapor compositions as well as geometries of a predominant enol form. The differences in some bond distances and bond angles are larger than their experimental uncertainties. This is not surprising, since two GED studies^{22,23} resulted in C_{2v} structures of the enol form. The structural parameters of the enol form obtained in this study are closest to the values reported by Srinivasan et al.,²⁵ excluding $r(\text{C3}-\text{O2})$. It should be noted that the parameters obtained in ref 25 (r_e) and in this work (r_{h1}) possess a different physical meaning. Unfortunately, the authors²⁵ do not describe the procedure of obtaining r_e from GED data; therefore, we have no possibility for a correct comparison of the structural parameters from ref 25 and our work. X-ray studies at two different temperatures⁴⁴ demonstrate that acetylacetone in a crystal exists in the cis-enolic form with the central hydrogen atom equally distributed over two positions near the oxygens.

Table 4. Conditions of GED/MS Experiments

	1 series		2 series	
nozzle to plate dist, mm	338	598	338	598
fast electron beam, μA	1.52	0.49	1.61	0.44
temp of effusion cell, K	301(5)	299(5)	677(5)	664(5)
accelerating voltage, kV	73.4	72.4	72.0	71.8
electron wavelength, \AA	0.04375(7)	0.04406(5)	0.04422(9)	0.04426(3)
ionization voltage, V	50	50	50	50
exposure time, s	60–100	50–55	100	50
residual gas pressure, Torr	2.3×10^{-6}	3.8×10^{-6}	1.5×10^{-6}	5.0×10^{-6}
s value range, \AA^{-1} ^a	2.2–26.6	1.1–13.8	3.1–26.5	1.2–13.8

^a $s = (4\pi/\lambda) \sin \theta/2$; λ is the electron wavelength, and θ is the scattering angle.

Table 5. Mass Spectral Data Recorded Simultaneously with GED Data for Acetylacetone

m/e	ion	abundance I , %	
		$T = 300\text{K}$	$T = 671\text{K}$
100	$[\text{M}]^+{}^a$	30.0	11.6
85	$[\text{M} - \text{CH}_3]^+$	38.9	19.0
72	$[\text{M} - \text{CO}]^+$	2.5	7.2
58	$[\text{M} - \text{C}(\text{O})\text{CH}_2]^+$	6.0	8.3
42	$[\text{C}(\text{O})\text{CH}_2]^+$	72.9	100
15	$[\text{CH}_3]^+$	100	80.2

^aDistances in \AA and angles in degrees. For atom numbering see Figure 1. ^bAverage values, corresponding to the superposition of two enol isomers. ^cB3LYP/aug-cc-pVTZ.

Thus, it is assumed that the X-ray structure of acac is a superposition of two nondistinguishable cis-enolic isomers with localized O–H bonds. The X-ray value of $r(\text{O}\cdots\text{O})$ is in agreement with our GED values and with the calculated values (see Table 3).

Table 3 shows that the structures of the diketo form obtained in the present study and in ref 22 are very different. According to the results of the earlier study,²² the distance $r(\text{O}\cdots\text{O})$ in the diketo form is 2.767(30) \AA and the dihedral O1C2C3O2 angle (48.6°) is rather strange. Our GED study results in $r(\text{O}\cdots\text{O}) = 4.051(43)$ \AA and $\text{O1C2C3O2} = 132.9(11.6)^\circ$ (the uncertainty is estimated from the uncertainties of O1C2C1C3) in the diketo form. These values can be compared with calculated (B3LYP/aug-cc-pVTZ) values: 4.042 \AA and 140.5° , respectively. The most recent study by Srinivasan et al.²⁵ does not contain details about the structure of the diketo form.²⁵ The reported $\text{O}\cdots\text{O}$ distance of 3.520 \AA and the dihedral O1C2C3O2 angle of 104.7° differ strongly from our experimental and calculated results. The reason for the difference could be connected to the procedure of GED data analysis applied by the authors of ref 25. Their attempt to refine the tautomer population using DFT structures at the start of structural analysis yielded an enol to keto ratio which is in contrast to that expected at the experimental temperature²⁵ according to NMR, UV, and IR studies. To avoid this discrepancy, in the first step the geometry of the keto form, which is free to undergo internal rotation about its C–C single bonds, was optimized using a fixed ratio of the tautomers. Refitting the equilibrium population using this modified keto structure resulted in a keto–enol ratio corresponding to the literature data.¹⁴ A structural refinement of the enol was then performed using the fit values for the equilibrium ratio and keto geometry.²⁵

Figure 3 presents a calculated potential curve for the position of the hydrogen atom between two oxygen atoms in the enol

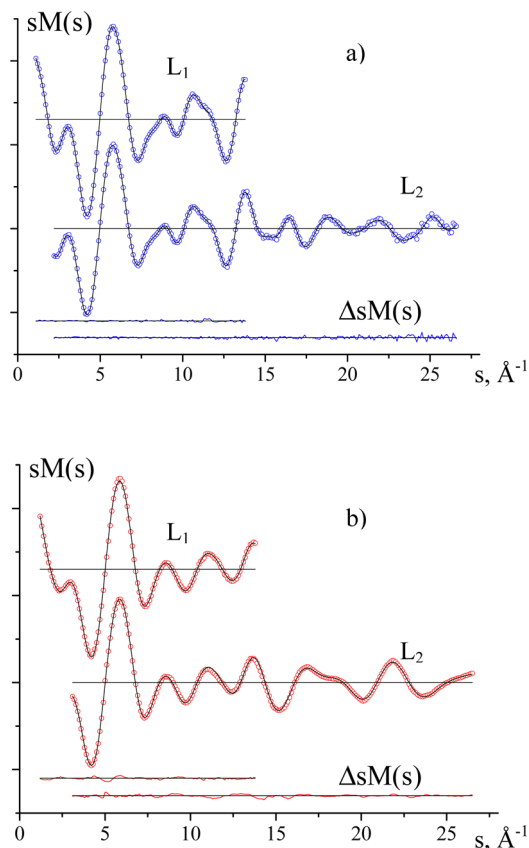


Figure 4. Experimental (dots) and calculated (solid lines) modified molecular intensity curves and residuals (experimental–theoretical) at two nozzle to plate distances ($L_1 = 598$ mm, $L_2 = 338$ mm) for two series of GED experiments: (a) $T = 300$ K; (b) $T = 671$ K.

form derived by B3LYP/6-31G(d,p) calculations. Two equivalent minima occur for localized hydrogen bonds with $r(\text{O}–\text{H}) = 1.018$ \AA : the maximum for $r(\text{O1}\cdots\text{H}) = r(\text{O2}\cdots\text{H}) = 1.206$ \AA . The height of this barrier is 1.67 kcal/mol. Transfer of the proton from O1 to O2 involves rotation of both methyl groups. In a transition state both methyl groups eclipse CC bonds. The proton transfer in acac was the subject of different studies. As was mentioned above, the value of the $\text{C}_s–\text{C}_{2v}–\text{C}_s$ barrier depends strongly on the computational method. High-level quantum chemical calculations (CCSD(T)/aug-cc-pVDZ) of fully relaxed geometry²⁶ yield a height of this barrier equal to 3.65 kcal/mol. Thus, one can conclude that the value of the proton transfer barrier is low enough to allow an exchange of a

hydrogen position during the X-ray diffraction experiment at room temperature. Furthermore, the properties of the O–H...O group in the crystal may differ from those of a free molecule due to intermolecular hydrogen bonds between neighboring molecules. According to an IR study³³ the value for $\nu(\text{O–H})$ of about 2800 cm^{-1} (gas phase and liquid) suggests the presence of a strong intramolecular hydrogen bond with a predominantly localized position of the enolic H atom. Thus, the theoretical and experimental results lead to the conclusion that the asymmetric C_s equilibrium structure of the enol form of acetylacetone is present. The discrepancy between this result and a microwave spectroscopic (MW) study,³⁵ where rotational transitions of a C_{2v} -symmetric enol are observed, could be due to different time scales in GED and MW experiments. Whereas the characteristic time scale (interaction of an electron with a molecule) in GED experiments is about 10^{-18} – 10^{-17} s, the time scale in MW spectroscopy is 10^{-11} – 10^{-10} s. During this time rapid exchange of hydrogen between two oxygen atoms can occur many times, resulting in average C_{2v} symmetry.

EXPERIMENTAL SECTION

A commercial sample (Aldrich 99+%) was used in GED experiments. The electron diffraction patterns and the mass spectra were recorded simultaneously using the techniques described previously.^{45,46} Two series of GED/MS experiments at two different vapor temperatures of acac were performed. The conditions of GED/MS experiments and the relative abundance of the characteristic ions of acetylacetone are shown in Tables 4 and 5, respectively. The main ions in mass spectra are equal to the literature data for acac.⁴¹ The inlet system was used for inserting vapor into the effusion cell. The temperature of the stainless steel effusion cell was measured by a W/Re-5/20 thermocouple calibrated by the melting points of Sn and Al. The wavelength of electrons was determined from the diffraction patterns of polycrystalline

ZnO. Optical densities were measured by a computer-controlled MD-100 (Carl Zeiss, Jena) microdensitometer.⁴⁷ The experimental and theoretical intensities $sM(s)$ are compared in Figure 4. Figure 5 presents the mass spectra recorded simultaneously with GED data.

ASSOCIATED CONTENT

Supporting Information

Table S1, giving interatomic distances, vibrational amplitudes, and vibrational corrections for the enol tautomer (excluding nonbonded distances involving hydrogen), Table S2, giving interatomic distances, vibrational amplitudes, and vibrational corrections for the diketo tautomer (excluding nonbonded distances involving hydrogen), and tables giving the results of MP2 and B3LYP calculations with different basis sets, including Cartesian coordinates, electronic energies, number of imaginary frequencies, zero point corrections, and thermal corrections to energies, enthalpies, and Gibbs free energies for the enol and diketo conformers. This material is available free of charge via the Internet at <http://pubs.acs.org>.

AUTHOR INFORMATION

Corresponding Author

*E-mail for N.V.B.: belova@isuct.ru.

Notes

The authors declare no competing financial interest.

ACKNOWLEDGMENTS

This work was supported by the Deutsche Forschungsgemeinschaft, by the Fonds der Chemischen Industrie, and by the Russian-German Cooperation Project (Russian Foundation for Basic Research Grant No. 12-03-91333-NNIO_a and DFG OB 28/22-1). We thank the editor R. J. McMachon and the two reviewers for valuable comments.

REFERENCES

- (1) Gomez-Garibay, F.; Calderon, J. S.; Quijano, L.; Tellez, O.; Socorro-Olivares, M.; Rios, T. *Phytochemistry* **2001**, 46 (7), 1285.
- (2) Wetz, F.; Routaboul, C.; Lavabre, D.; Garrigues, J. C.; Rico-Latters, I.; Pernet, I.; Denis, A. *Photochem. Photobiol.* **2004**, 80, 316.
- (3) Emsley, J. In *Complex Chemistry*; Springer-Verlag: Berlin, 1984; Structure and Bonding Vol. 57, p 147.
- (4) Schwach, W.; Rudolph, T. *J. Photochem. Photobiol. B: Biol.* **1995**, 28 (3), 229.
- (5) Tanaka, M.; Shono, T.; Shinra, K. *Bull. Chem. Soc. Jpn.* **1969**, 42, 3190.
- (6) Zhang, B. L.; Mabon, F.; Martin, M. L. *J. Phys. Org. Chem.* **1993**, 6, 367.
- (7) Harries, H. J.; Parry, G.; Burgess, J. *Inorg. Chim. Acta* **1978**, 31, 233.
- (8) Burdett, J. L.; Rogers, M. T. *J. Am. Chem. Soc.* **1964**, 86 (11), 2105.
- (9) Grushow, A.; Zielinski, T. J. *J. Chem. Educ.* **2002**, 79 (6), 707.
- (10) Bunting, J. W.; Kanter, J. P.; Nelander, R.; Wu, Z. *Can. J. Chem.* **1995**, 73, 1305.
- (11) Karabulut, S.; Namli, H. *J. Mol. Struct.* **2012**, 1024, 151.
- (12) Temprado, M.; Roux, M. V.; Umnahanant, P.; Zhao, H.; Chickos, J. S. *J. Phys. Chem. B* **2005**, 109, 12590.
- (13) Irving, R. J.; Wadso, I. *Acta Chem. Scand.* **1970**, 24, 589.
- (14) Folkendt, M. M.; Weiss-Lopez, B. E.; Chauvel, J. P.; True, N. S. *J. Phys. Chem.* **1985**, 89, 3347.
- (15) Roubin, P.; Chiavassa, T.; Pizzala, P.; Bodot, H. *J. Chem. Phys. Lett.* **1990**, 175 (6), 655.
- (16) Trivella, A.; Wassermann, T. N.; Mestdagh, J. M.; Manca Tanner, C.; Marinelli, F.; Roubin, P.; Coussan, S. *Phys. Chem. Chem. Phys.* **2010**, 12, 8300.

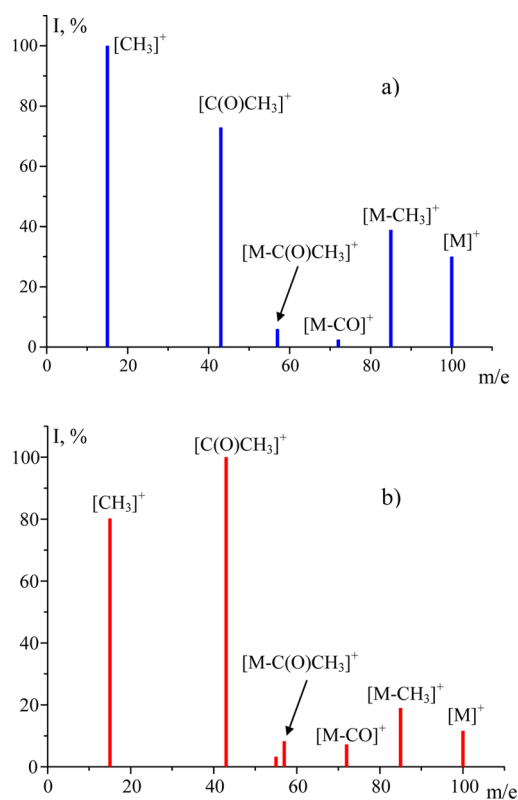


Figure 5. Mass spectra recorded simultaneously with GED patterns: (a) $T = 300\text{ K}$; (b) $T = 671\text{ K}$.

- (17) Lozada-Garcia, R. R.; Ceponkus, J.; Chin, W.; Chevalier, M.; Crepin, C. *Chem. Phys. Lett.* **2011**, 504, 142.
- (18) Schweig, A.; Vermeer, H.; Weidner, U. *Chem. Phys. Lett.* **1974**, 26 (2), 229.
- (19) Cabral do Couto, P.; Costa Cabral, B. J.; Martinho Simoes, J. A. *Chem. Phys. Lett.* **2006**, 419, 486.
- (20) Bauer, S. H.; Wilcox, C. F. *Chem. Phys. Lett.* **1997**, 279, 122.
- (21) Sliznev, V. V.; Lapshina, S. B.; Girichev, G. V. *J. Struct. Chem.* **2006**, 47 (2), 220.
- (22) Lowrey, A. H.; George, C.; D'Antonio, P.; Karle, J. J. *Am. Chem. Soc.* **1971**, 93 (24), 6399.
- (23) Andreassen, A. L.; Bauer, S. H. *J. Mol. Struct.* **1972**, 12, 381.
- (24) Iijima, K.; Ohnogi, A.; Shibata, S. *J. Mol. Struct.* **1987**, 156, 111.
- (25) Srinivasan, R.; Feenstra, J. S.; Park, S. T.; Xu, S.; Zewail, A. H. *J. Am. Chem. Soc.* **2004**, 126, 2266.
- (26) Broadbent, S. A.; Burns, L. A.; Chatterjee, C.; Vaccaro, P. H. *Chem. Phys. Lett.* **2007**, 434, 31.
- (27) Rios, M. A.; Rodriguez, J. G. *J. Mol. Struct. (THEOCHEM)* **1990**, 204, 137.
- (28) Dannenberg, J. J.; Rios, R. *J. Phys. Chem.* **1994**, 98, 6714.
- (29) Barich, D. H.; Nicholas, J. B.; Haw, J. F. *J. Phys. Chem. A* **2001**, 105, 4708.
- (30) Campomanes, P.; Menendez, M. I.; Sordo, T. L. *J. Mol. Struct. (THEOCHEM)* **2005**, 713, 59.
- (31) Matanovic, I.; Doslic, N. *Int. J. Quantum Chem.* **2006**, 106, 1367.
- (32) Sliznev, V. V.; Lapshina, S. B.; Girichev, G. V. *J. Struct. Chem.* **2002**, 43 (1), 51.
- (33) Tayyari, S. F.; Milani-nejad, F. *Spectrochim. Acta, Part A* **2000**, 56, 2679.
- (34) Belova, N. V.; Sliznev, V. V.; Oberhammer, H.; Girichev, G. V. *J. Mol. Struct.* **2010**, 978, 282.
- (35) Caminati, W.; Grabow, J.-U. *J. Am. Chem. Soc.* **2006**, 128 (3), 854.
- (36) Frisch, M. J.; Trucks, G. W.; Schlegel, H. B.; Scuseria, G. E.; Robb, M. A.; Cheeseman, J. R.; Montgomery, J. A., Jr.; Vreven, J. T.; Kudin, K. N.; Burant, J. C.; Millam, J. M.; Iyengar, S. S.; Tomasi, J.; Barone, V.; Mennucci, B.; Cossi, M.; Scalmani, G.; Rega, N.; Petersson, G. A.; Nakatsuji, H.; Hada, M.; Ehara, M.; Toyota, K.; Fukuda, R.; Hasegawa, J.; Ishida, M.; Nakajima, T.; Honda, Y.; Kitao, O.; Nakai, H.; Klene, M.; Li, X.; Knox, J. E.; Hratchian, H. P.; Cross, J. B.; Adamo, C.; Jaramillo, J.; Gomperts, R.; Stratmann, R. E.; Yazyev, O.; Austin, A. J.; Cammi, R.; Pomelli, C.; Ochterski, J. W.; Ayala, P. Y.; Morokuma, K.; Voth, G. A.; Salvador, P.; Dannenberg, J. J.; Zakrzewski, V. G.; Dapprich, S.; Daniels, A. D.; Strain, M. C.; Farkas, O.; Malick, D. K.; Rabuck, A. D.; Raghavachari, K.; Foresman, J. B.; Ortiz, J. V.; Cui, Q.; Baboul, A. G.; Clifford, S.; Cioslowski, J.; Stefanov, B. B.; Liu, G.; Liashenko, A.; Piskorz, P.; Komaromi, I.; Martin, R. L.; Fox, D. J.; Keith, T.; Al-Laham, M. A.; Peng, C. Y.; Nanayakkara, A.; Challacombe, M.; Gill, P. M. W.; Johnson, B.; Chen, W.; Wong, M. W.; Gonzalez, C.; Pople, J. A. *Gaussian 03*; Gaussian, Inc., Pittsburgh, PA, 2003.
- (37) Sipachev, V. A. *J. Mol. Struct.* **2001**, 567–568, 67.
- (38) Sipachev, V. A. *J. Mol. Struct. (THEOCHEM)* **1985**, 121, 143.
- (39) Sipachev, V. A. In *Advances in Molecular Structure Research*; Hargittai, I., Hargittai, M., Eds.; JAI Press: New York, 1999; Vol. 5, p 263.
- (40) Hamilton, W. C. *Acta Crystallogr.* **1965**, 18, 502.
- (41) Zamir, L.; Jensen, B. S.; Larsen, E. *Org. Mass Spectrom.* **1969**, 2, 49.
- (42) Belova, N. V.; Girichev, G. V.; Shlykov, S. A.; Oberhammer, H. *J. Org. Chem.* **2006**, 71, 5298.
- (43) Belova, N. V.; Oberhammer, H.; Girichev, G. V. *J. Phys. Chem. A* **2004**, 108, 3593.
- (44) Boese, R.; Antipin, M. Y.; Blaser, D.; Lyssenko, K. A. *J. Phys. Chem. B* **1998**, 102, 8654.
- (45) Girichev, G. V.; Utkin, A. N.; Revichev, Y. F. *Instrum. Exp. Tech.* **1984**, 27 (2), 457.
- (46) Girichev, G. V.; Shlykov, S. A.; Revichev, Y. F. *Instrum. Exp. Tech.* **1986**, 29 (4), 939.
- (47) Girichev, E. G.; Zakharov, A. V.; Girichev, G. V.; Bazanov, M. I. *Izv. Vyssh. Uchebn. Zaved., Tekhnol. Tekst. Prom-sti.* **2000**, 2, 142.